Quantum Dot Labelling of Adenovirus Allows for Highly Sensitive Single Cell Flow and Imaging Cytometry

*Morgan R. Herod, Robert G. Pineda, Vivien Mautner and David Onion**

Dr. Morgan R. Herod. School of Molecular and Cellular Biology, Faculty of Biological Sciences, University of Leeds, Leeds, LS2 9JT, UK.

Mr. Robert G. Pineda. Tumour and Vascular Biology Labs, Cancer Biology, School of Medicine, University of Nottingham, Nottingham, NG7 2UH, UK.

Dr. Vivien Mautner School of Cancer Sciences, University of Birmingham, Birmingham, B15 2TT, UK.

Dr. David Onion University of Nottingham Flow Cytometry Facility, School of Life Sciences, University of Nottingham, NG7 2UH, UK.

E-mail: david.onion@nottingham.ac.uk

Genetic modification of adenoviral capsid proteins is a commonly used strategy for broadening the tissue tropism of adenoviral gene therapy vectors and thus increasing their therapeutic potential. To accurately measure the effects on cell tropism of genetically modified adenovirus vectors, new highly sensitive detection and tracking techniques are required that can be easily adapted to the wide array of pre-existing gene therapy vectors without the need for further genetic modification. Quantum dots are nano-sized fluorescent particles with high quantum yields and extended photo-stability, making them excellent labels for single particle detection. We have utilised streptavidin-conjugated quantum dot technology to detect the binding of biotinylated human adenovirus and adenoviral gene

therapy vectors to target cells. We demonstrate that this technique has no impact on virus fitness or specificity whilst enabling the detection of virus binding events and internalisation using a variety of imaging and cytometry techniques. Furthermore, Qdot labelling of adenovirus is at least 10-fold more sensitive than conventional organic fluorophore labelling techniques such as genetic incorporation of eGFP into the viral capsid. This method has been applied to characterise the tropism of different adenovirus species and tropism-modified adenoviral gene therapy vectors and will provide a valuable new tool for studying adenoviral receptor interaction and cell entry.

The seven species of human adenovirus (A-G) comprise at least 52 serotypes which are responsible for a range of usually mild and self-limiting infections. Most species A, C, E, F and G human adenoviruses (Ad) and some from species D can bind to cells via interaction of the fibre knob domain with the coxsackie and adenovirus receptor (CAR).[1-3] Species C adenoviruses have also been reported to use heparan sulphate glycosaminoglycans (HSGs)[4, 5] as primary receptors and are able to bind heparan sulphate proteoglycans via a bridging interaction with factor X,[6, 7] dipalmitoyl phosphatidylcholine[8] or lactoferrin[9]. CD46 has been identified as the primary receptor for species B viruses (except 3 and 7 which use desmoglein-2)[10-12] and sialic acid the primary receptor for most species D viruses responsible for epidemic keratoconjunctivitis.[13-15] Following initial cell attachment, internalisation is mediated in most cases by penton base binding to $\alpha_V\beta_3$ or $\alpha_V\beta_5$ integrins.[16] Numerous human and non-human Ad serotypes have been developed for gene delivery and in addition many have been tropism modified either genetically or chemically to improve gene delivery to target cells.[17] Given the array of different viruses and cellular receptors, highly sensitive techniques to track virus and define virus-cell binding

interactions are valuable in understanding the natural viral lifecycle as well as in the development of new gene delivery vectors.

Quantum dots (Qdots) are nano scale particles which can be used as fluorescent labels of biological molecules.[18-20] They are composed of an inorganic core, which determines the fluorescent properties, surrounded by a shell of zinc sulphide to improve optical properties and prevent leaching and further encompassed by an organic layer allowing dispersion in water. Qdots have a blue shifted excitation profile, high quantum yield, discrete emission spectrum (determined by the size of the inorganic core) and are highly photo-stable,[21] features which offer significant advantages over organic fluorophores. Binding of Qdots to the recipient biological molecule first requires surface functionalisation of both the Qdot and the target molecule. In the context of labelling adenovirus, chemical surface functionalisation may provide advantages over genetic functionalisation, as genetically modified capsid components can be detrimental to virus fitness and genetic stability. The minor capsid protein pIX has been identified as an attractive target for genetic modification[22], however both replication deficient[23] and replication competent viruses bearing pIX-GFP fusions have significantly compromised fitness.[24, 25] As an alternative method, Ad has been chemically surface modified with fluorophores such as Texas Red (TR).[26] TR-succidmyl esters react with free amino groups on the surface of the virus capsid, covalently attaching the fluorophore to purified virus in a simple one step reaction. Texas Red labelled virus has been used to analyse virus binding and sub-cellular trafficking, however this is a process which requires complex image acquisition, analysis and suffers from photo-bleaching and low levels of sensitivity. Qdots have been used to label a range of different viruses[27-38] including enveloped viruses such as human T cell leukaemia virus (HTLV)[39] and human immunodeficiency virus (HIV),[40] non-enveloped viruses such as adeno-associated virus (AAV)[41] and have been incorporated into SV40 pseudoparticles[42]

Furthermore, Qdots have been recently utilised as highly sensitive reagents for the detection of medically relevant pathogens[43-47] including hepatitis B virus[48, 49], Epstein-Barr virus[50-52] and picornaviruses,[53, 54] and have therefore been suggested as potential tools in medical diagnosis.

In this study we describe a method to label adenovirus with streptavidin functionalised Qdots following chemical biotinylation of the virion surface proteins. The technique is rapid, reproducible, and can be applied to different serotypes and to tropism modified vectors. Labelling does not interfere with virus fitness and its application in studying virus internalisation and trafficking is demonstrated using imaging cytometry.

In order to determine the level of biotinylation compatible with retention of virus viability, a replication deficient Ad vector expressing eGFP (AdGFP)[55] which had been purified [56] was chemically biotinylated by incubation with increasing concentrations of N-hydroxysuccinimido-biotin (NHS-biotin) (10, 100 and 1000 μg/ml for 4 hours, room temperature) and free NHS-biotin removed by dialysis. Biotinylated virus was used to infect A549 cells (a cell line expressing high levels of CAR and permissive to Ad replication) at 100 particles/cell and transduction assessed by GFP expression measured at 48 hours post infection by flow cytometry (Figure 1 (A)). The highest concentration (1 mg/ml) of biotin led to a complete block in virus transduction, presumably due to biotin interfering with fiber-CAR interactions, whilst at 100 μg/ml there was a 200-fold reduction in gene expression relative to unmodified virus. However at 10 μg/ml, over 90% of transduction efficiency was retained. Concordant with this, virus particle to infectivity ratio of 10 μg/ml biotinylated Ad was slightly higher than unmodified virus (15:1 vs 10:1, data not shown) but still within the acceptable range for adenoviral gene delivery vectors (typically between 10:1

and 100:1). Therefore for all subsequent work viruses were biotinylated with 10 μg/ml NHS-Biotin.

Qdots display on their surface quadrivalent streptavidin and conjugating them directly to free biotinylated adenovirus in suspension led to virus aggregation and inactivation (data not shown); we therefore chose to bind virus to the cells prior to Qdot labelling. Furthermore, cells were pre-treated with excess biotin and streptavidin (as described in material and methods), to further reduce non-specific binding events.

To label virus with Qdots, 10^5 cells were incubated with increasing multiplicity of infection (MOI) of biotinylated AdGFP (bAdGFP) in the range 1 – $1x10^5$ particles/cell (90 minutes on ice), or mock infected and labelled with Qdots (1μl of Qdot655-streptavidin conjugate/50 μl, 60 minutes on ice) and analysed by flow cytometry (Figure 1 (B)). As anticipated, Qdot fluorescence increased with increasing virus MOI, no appreciable fluorescence was detected with mock infected Qdot labelled cell above completely unlabelled cells.

In order to compare the sensitivity of Qdot labelling with that of viral capsid bearing an organic fluorophore, the experiment was performed in parallel with a virus which encoded a pIX-GFP fusion protein (AdpIX-GFP):[23] with each virus capsid containing up to 240 copies of the pIX-GFP- fusion protein (Figure 1 (B)). While two viruses were of the same serotype and had comparable particle[57] to infectivity ratio the GFP fluorescence of AdpIX-GFP, was not readily detectable below 10^4 particles/cells indicating the GFP tagging was in the order of 10-fold less sensitive than the Qdot labelling technique. Furthermore, the mean fluorescence yield for Qdot labelling was approximately 100-fold higher than that of GFP labelling at the same MOI (data not shown). To determine whether the labelling was bright

enough to detect single virus binding events by fluorescence microscopy, A549 cells were incubated with bAdGFP and Qdot655 labelled before being counterstained with DAPI and anti-CAR antibody (Figure 1 (C and D)). Fluorescent confocal microscopy revealed distinct foci consistent with individual virus binding events.

To determine whether biotinylation or Qdot labelling adversely altered virus attachment, binding experiments were performed using A9-CAR cells[58] (murine fibroblasts stably expressing human chromosome 21 which encodes human CAR) and parental A9 cells which are devoid of CAR, HSGs and α_V integrins and thus are totally refractory to wild type Ad5 binding and infection.[58] A9-CAR and A9 cells pre-treated with excess biotin and streptavidin were mixed at a ratio of 2:1 before virus and Qdot were bound on ice; cells were then stained for CAR expression and analysed by flow cytometry (Figure 2 (A)). Only CAR positive cells showed Qdot fluorescence after incubation with bAdGFP, whereas all cells incubated with AdGFP were negative for Qdot fluorescence. This confirms that the Qdot fluorescence is bAdGFP specific, that the biotinylation has not caused non-specific binding to a receptor negative cell line, and that the biotinylated virus can still bind to cells bearing an appropriate receptor.

In order to determine whether biotinylation and labelling would compromise the ability of virus to internalise, A549 cells were incubated with bAdGFP and Qdots on ice to allow binding, before incubation at 37°C to allow internalisation. Cells were fixed in ice cold formaldehyde at regular time intervals up to 180 minutes and analysed by imaging cytometry (>4000 in focus single cell events per time point). For each cell analysed the internalised fluorescence was expressed relative to the total cell fluorescence and values normalised to the maximal internalisation achieved in the experiment (Figure 2 (B)).

bAdGFP internalisation was rapid, with 50% achieved within 5 minutes and the maximum (>95% internalised virus) achieved by 60 minutes. Figure 2 (C) shows the location of Qdot655 staining on representative images from the 0, 30, 60 and 180 minute timepoints. Qdot fluorescence was almost entirely associated with the plasma membrane at the 0 minute timepoint, after 30 minutes at 37°C virus fluorescence was entirely interior to the plasma membrane, at 60 minutes the fluorescence was mostly cytoplasmic and by 180 minutes there was distinct peri-nuclear accumulation of label, consistent with the ability of Qdot labelled virus to efficiently bind, internalise, and accumulate at the nuclear envelope.

In order to demonstrate biotinylation/Qdot labelling can be applied to different adenovirus species; WTAd5 (species C) and WTAd11 (species B) were biotinylated and Qdot labelled. To test a tropism modified gene therapy vector, AdDM-1/E2F-RGD, an Ad5 derived oncolytic adenovirus vector genetically retargeted by incorporating the RGD α_V integrin binding motif in the fiber HI loop, and an equivalent non-fiber modified vector AdDM-1/E2F, were also tested. The efficiency of binding was determined on the human ovarian tumour cell line SKOV3 (which are low for CAR expression, but CD46 positive) and the matched cell line SKOV3-CAR[59] (which stably expresses human CAR). bAd5, bAd11, bAdDM-1/E2F and bAdDM-1/E2F-RGD were titrated onto SKOV3 and SKOV3-CAR cells at 4°C, before Qdot655 labelling and analysis by flow cytometry (Figure 3). All four viruses displayed a dose dependent increase in fluorescence on both cell lines. Approximately 10-fold more bAd5 was required on SKOV3 cells to achieve the same fluorescence as on SKOV3-CAR cells, indicating its high preference for CAR binding (Figure 3A). Both bAd11 and bAd5 show similar binding levels on SKOV3-CAR cells, both serotypes reaching saturation at 10^4 particles/cell. However, bAd11 bound to SKOV3 and SKOV3-CAR cells with equal efficiency as they both express its primary receptor CD46 (Figure 3B),

whereas Ad5 showed significantly lower levels of binding to SKOV3 than SKOV3-CAR. Introduction of the RGD integrin binding motif into Ad5 fiber has previously been reported to increase the efficiency of binding of Ad5 to CAR negative cells lines.[60, 61] The binding of bAdDM-1/E2F (with WT Ad5 fiber) to SKOV3 and SKOV3-CAR cells showed a similar profile to that of bAd5 (Figure 3C), with significantly less virus binding the SKOV3 cells than the SKOV-CAR cells. However, the RGD modified vector, bAdDM-1/E2F-RGD, demonstrated improved binding efficiency on the CAR negative SKOV3 cells with no significant differences in binding detected between the two cell lines irrespective of CAR expression (Figure 3D).

The unique optical properties of Qdots[18, 19] make them an attractive label for virus particle tracking. The brightness of emission permits detection of single virus particles using conventional fluorescent imaging technology such as confocal microscopy. Their inherent photo-stability facilitates data acquisition, with reduced photo-bleaching, and offers major advantages for virus tracking in live cells where the same cell comes under laser illumination multiple times or continuously.[62] Kampani *et al* used Qdots to label HTLV[39] and demonstrated that increased virus binding was proportional to increased fluorescence, and therefore could be used for virus titration. Subsequently Joo *et al* applied a similar strategy to label lysates of HIV infected cells to analyse virus binding to lymphocytes,[40] and SV40-Qdot hybrid pseudoparticles have been constructed allowing for imaging of virus binding and internalisation by time lapse confocal microscopy.[42] Since these initial studies Qdots have been used to label a number of enveloped and non-enveloped viruses,[29, 31, 37, 41, 63] allowing for single virus tracking of baculovirus,[27, 30] influenza A virus[32, 64] and hematopoietic necrosis virus[35] which has facilitated a more detailed characterisation of viral endocytitic pathways.

Here we show for the first time Qdots can be conjugated to intact adenoviruses without a detrimental impact or modification of viral function, tropism, internalisation or transduction efficacy. Furthermore, this quantum dot Ad labelling technique was at least 10-times more sensitive than an Ad5 displaying surface eGFP, genetically fused to the viral capsid. In combination with imaging cytometry analysis, the Qdot labelling strategy described here can be easily used to visualise and accurately measure virus internalisation.

Adenovirus internalisation and sub-cellular trafficking has previously been studied using both transmission electron microscopy (TEM)[65] and fluorescent labelling with texas red.[26] TEM is a relatively laborious and time consuming technique, with analysis usually performed on a small number of cells. Similarly, the image acquisition and analysis for Texas Red labelled Ad involves Fourier transformation of multiple Z sections of individual cells taken with a CCD camera under high magnification and as a consequence analysis is limited to a relatively small number of cells. Imaging cytometric analysis is an emerging technology which combines the high throughput and statistical rigour of flow cytometry with the locational information provided by fluorescent microscopy.[66] Here we were able to measure virus internalisation rapidly and reproducibly, acquiring and analysing data for thousands of cells at multiple time points. Internalisation of virus pre-bound to A549 cells was rapid, with greater than 50% of virus internalised within 5 minutes. By 180 minutes post-infection, much of the Qdot fluorescence was concentrated around the nucleus which is similar to the rate at which virus escapes the endosome and traffics to the nucleus,[67-72] suggesting Qdots remain associated with the partially uncoated virus capsids. The Qdot labelling technique did not reduce virus infectivity as measured by plaque assay or the ability of transgene containing vectors to transduce target cell lines and so while

uncharacterised effects of Qdots on cellular uptake pathways cannot be ruled out, the normal productive viral pathways appears to be largely unperturbed. Whilst the number of Qdots bound to each viral particle is unclear from the data presented we anticipate based on the average diameter of an Adenovirus type 5 capsid (approximately 90nm) and the average diameter of the quantum dots used (approximately 15nm), a maximum Qdot to virus ratio of ~4:1. However it is important to note that for quantification, the binding should be uniform across each viral capsid and thus total mean fluorescence is proportional to amount of bound virus.

The Qdot labelling method we describe here is of value for the study of virus entry and sub-cellular localisation as well as for characterisation of the numerous tropism-modified gene delivery vectors under development. We demonstrate that the Qdot labelling strategy works equally well for Ad5 and Ad11, which use different cellular receptors (CAR and CD46, respectively), and for an Ad5 based gene therapy vector with the RGD integrin binding motif inserted in the HI loop of the fiber protein. All viruses bound to SKOV3-CAR cells with very similar efficiencies, whilst, as would be expected the WTAd5 fiber-containing viruses bound to SKOV3 (CAR negative) cells with a 10-fold reduced efficiency. It has previously been reported that insertion of an RGD motif within the HI loop of Ad5 vectors increases the binding to integrin positive human cells,[60] including SKOV3 cells,[61] primarily through interaction with $\alpha_V\beta_3$.[73] Consistent with this observation, AdDM-1/E2F-RGD bound CAR negative SKOV3 cells with only a slightly reduced (non-significant) efficiency relative to the CAR positive equivalent (SKOV-CAR) and with greater efficiency than the WT Ad5 fiber containing viruses (AdDM-1/E2F and WTAd5). Ad11 bound both SKOV3 and SKOV3-CAR cells with equal efficiency, consistent with their equal expression of CD46.

In conclusion, we demonstrate that quantum dot labelling is a sensitive technique to quantify cellular binding and uptake of adenovirus. This method will be useful for assessing the interaction of tropism modified gene therapy vectors with target and non-target cells to identify low level binding events. Furthermore, when in combination with imaging cytometry, Qdot labelling provides a simple method for studying viral internalisation and intra-cellular trafficking.

Acknowledgement

This work was supported by a University Hospital Birmingham (UHB) Charities Medical studentship M.R.H and a Medical Research Council (MRC), project grant V.M./D.O.

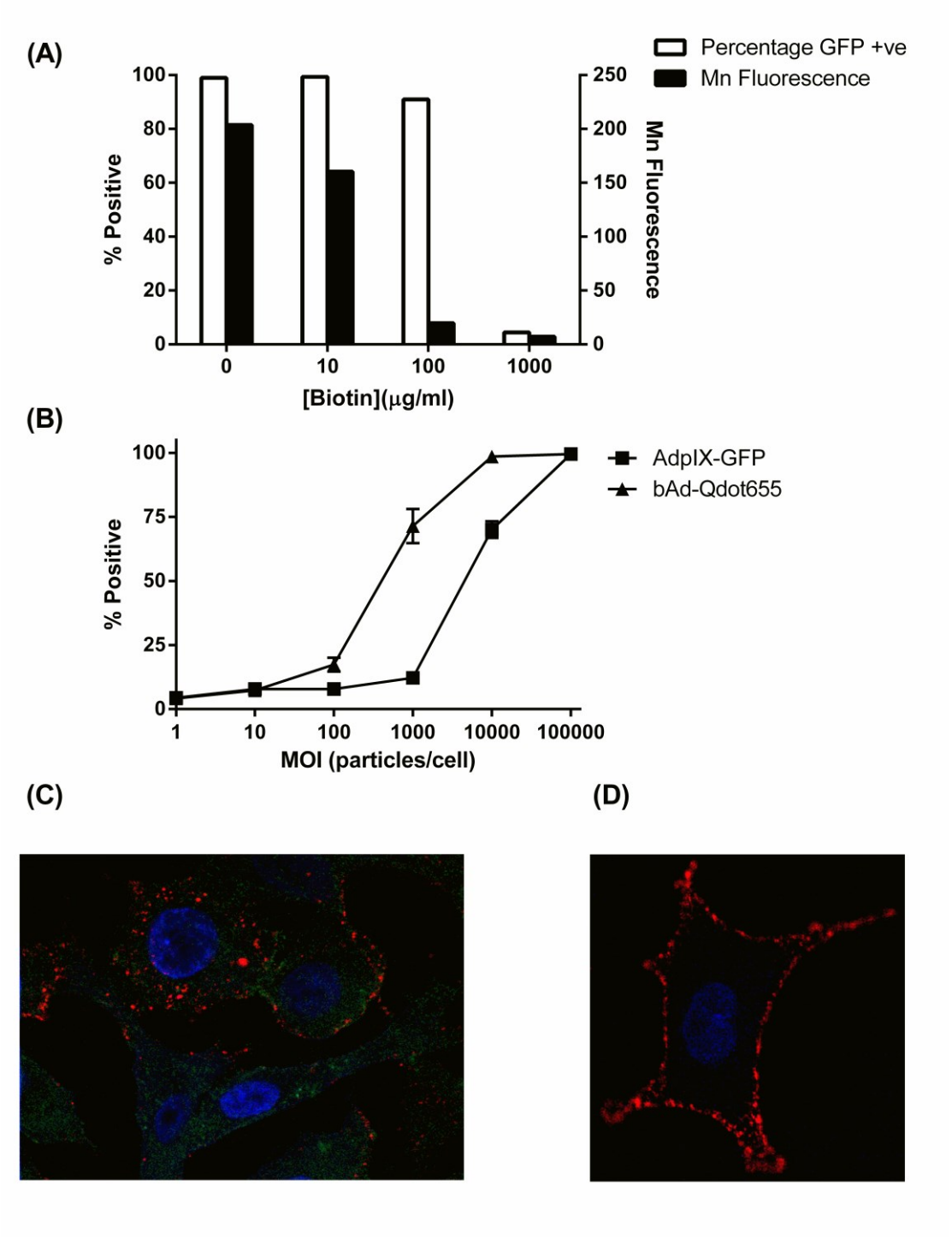

Figure 1 Quantum dot labelled biotinylated adenovirus. (A) Transduction of A549 cells with 100 particles/cell of biotinylated AdGFP as determined by flow cytometry 48 hours post infection (B) Comparison of Qdot655 labelled bAdGFP to pIX-GFP labelled AdpIX-GFP. A549 cells were infected with appropriate viruses at stated MOI (60 minutes, 4°C) and

Qdot655 added. Cells were analysed by flow cytometry to determine the percentage of cells with detectable GFP signal or Qdot655 signal in comparison to mock infected cells (data shows mean, n=3, +/- S.D.). (C and D) Representative confocal images of bAdGFP binding to A549 cells at 10^3 particles/cell showing a single confocal Z-section detected with anti-mouse Qdot525 secondary antibody co-stained with DAPI and anti-CAR RmCb (C) a composite stack of 10 optical Z-slices of a single cell counter-stained with DAPI (D). Images were taken with a 63X lens with 1.5X digital zoom.

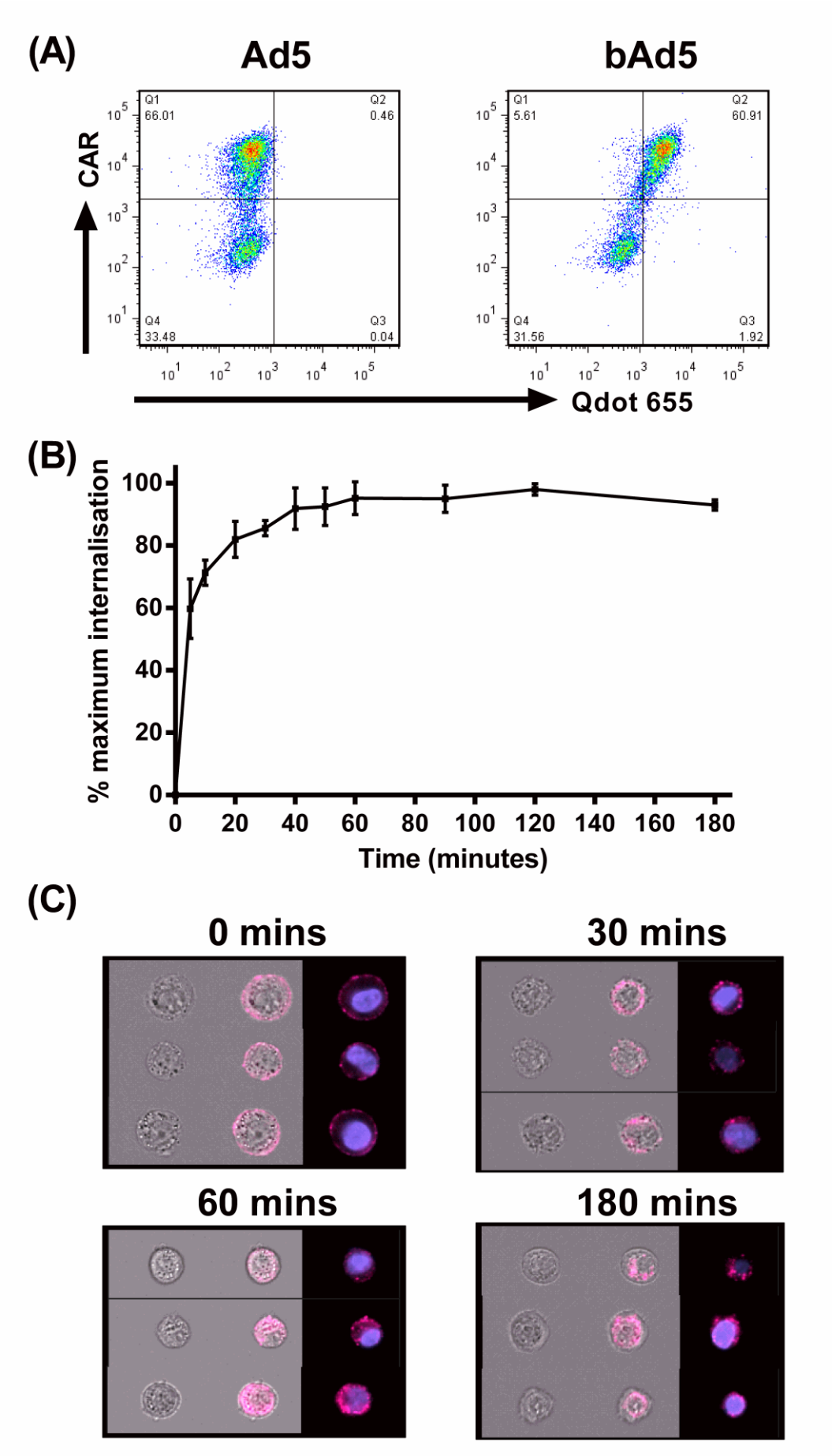
(A)
Ad5
bAd5
CAR
Qdot 655
Q1
66.01
Q2
0.46
Q4
33.48
Q3
0.04
Q1
5.61
Q2
60.91
Q4
31.56
Q3
1.92
(B)
% maximum internalisation
Time (minutes)
(C)
0 mins
30 mins
60 mins
180 mins

Figure 2 CAR specificity and internalisation of QdotbAd5 (A) A9-CAR and parental A9 cells were mixed at ratio of 2:1 and infected with Ad5 or bAd5 (60 minutes, 4°C, MOI 10^4 particles/cell), before addition of Qdot655 and co-staining with anti-CAR and anti-mouse FITC secondary, cells were analysed by flow cytometry. (B and C) A549 cells were infected with bAd5 (60 minutes, 4°C, MOI 10^4 particles/cell), cells were incubated at 37°C for the specified times before fixing in ice cold formaldehyde, counter-staining with DAPI and analysed using an Amnis image stream 100. (B) Normalised surface internalisation. Data shows mean, n=3, +/- S.D. (C) Representative images showing brightfield, brightfield merged with bAd5-Qdot655 fluorescence and bAd-Qdot655 fluorescence merged with DAPI staining.

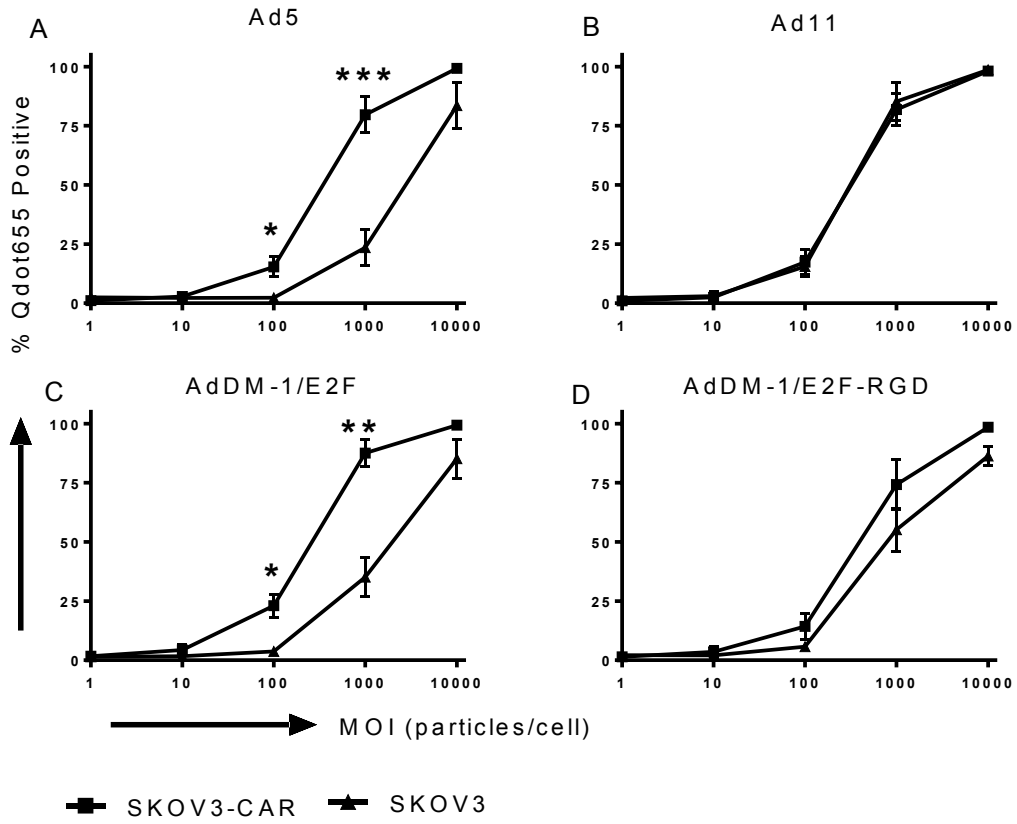

Figure 3. Qdot labelling of different Ad serotypes and tropism modified gene therapy vectors. Biotinylated (A) Ad5; (B) Ad11; (C) AdDM-1/E2F and (D) AdDM-1/E2F-RGD were bound to SKOV3 and SKOV3-CAR cells (on ice at given MOIs) before incubation with Qdot655 and analysis by flow cytometry (data shows mean, n=3, +/- S.D., * indicate significant differences between binding to SKOV-CAR and SKOV cells (Paired T Test)).

Reference List

[1] J. M. Bergelson, J. A. Cunningham, G. Droguett, E. A. Kurt-Jones, A. Krithivas, J. S. Hong, M. S. Horwitz, R. L. Crowell, R. W. Finberg, *Science* **1997,** *275*, 1320-1323.

[2] P. W. Roelvink, A. Lizonova, J. G. Lee, Y. Li, J. M. Bergelson, R. W. Finberg, D. E. Brough, I. Kovesdi, T. J. Wickham, *J. Virol.* **1998,** *72*, 7909-7915.

[3] R. P. Tomko, R. Xu, L. Philipson, *Proc. Natl. Acad. Sci. U. S. A* **1997,** *94*, 3352-3356.

[4] M. C. Dechecchi, A. Tamanini, A. Bonizzato, G. Cabrini, *Virology* **2000,** *268*, 382-390.

[5] M. C. Dechecchi, P. Melotti, A. Bonizzato, M. Santacatterina, M. Chilosi, G. Cabrini, *J. Virol.* **2001,** *75*, 8772-8780.

[6] O. Kalyuzhniy, N. C. Di Paolo, M. Silvestry, S. E. Hofherr, M. A. Barry, P. L. Stewart, D. M. Shayakhmetov, *Proc. Natl. Acad. Sci. U. S. A* **2008,** *105*, 5483-5488.

[7] S. N. Waddington, J. H. McVey, D. Bhella, A. L. Parker, K. Barker, H. Atoda, R. Pink, S. M. Buckley, J. A. Greig, L. Denby, J. Custers, T. Morita, I. M. Francischetti, R. Q. Monteiro, D. H. Barouch, N. van Rooijen, C. Napoli, M. J. Havenga, S. A. Nicklin, A. H. Baker, *Cell* **2008,** *132*, 397-409.

[8] L. Balakireva, G. Schoehn, E. Thouvenin, J. Chroboczek, *J. Virol.* **2003,** *77*, 4858-4866.

[9] C. Johansson, M. Jonsson, M. Marttila, D. Persson, X. L. Fan, J. Skog, L. Frangsmyr, G. Wadell, N. Arnberg, *J. Virol.* **2007,** *81*, 954-963.

[10] A. Gaggar, D. M. Shayakhmetov, A. Lieber, *Nat. Med.* **2003,** *9*, 1408-1412.

[11] M. Marttila, D. Persson, D. Gustafsson, M. K. Liszewski, J. P. Atkinson, G. Wadell, N. Arnberg, *J. Virol.* **2005,** *79*, 14429-14436.

[12] A. Segerman, J. P. Atkinson, M. Marttila, V. Dennerquist, G. Wadell, N. Arnberg, *J. Virol.* **2003,** *77*, 9183-9191.

[13] N. Arnberg, A. H. Kidd, K. Edlund, F. Olfat, G. Wadell, *J. Virol.* **2000,** *74*, 7691-7693.

[14] N. Arnberg, P. Pring-Akerblom, G. Wadell, *J. Virol.* **2002,** *76*, 8834-8841.

[15] W. P. Burmeister, D. Guilligay, S. Cusack, G. Wadell, N. Arnberg, *J. Virol.* **2004,** *78*, 7727-7736.

[16] T. J. Wickham, P. Mathias, D. A. Cheresh, G. R. Nemerow, *Cell* **1993,** *73*, 309-319.

[17] H. Bachtarzi, M. Stevenson, K. Fisher, *Expert. Opin. Drug Deliv.* **2008,** *5*, 1231-1240.

[18] M. Bruchez, Jr., M. Moronne, P. Gin, S. Weiss, A. P. Alivisatos, *Science* **1998,** *281*, 2013-2016.

[19] W. C. Chan, S. Nie, *Science* **1998,** *281*, 2016-2018.

[20] P. Facci, V. Erokhin, S. Carrara, C. Nicolini, *Proc. Natl. Acad. Sci. U. S. A* **1996,** *93*, 10556-10559.

[21] U. Resch-Genger, M. Grabolle, S. Cavaliere-Jaricot, R. Nitschke, T. Nann, *Nat. Methods* **2008,** *5*, 763-775.

[22] I. P. Dmitriev, E. A. Kashentseva, D. T. Curiel, *J. Virol.* **2002,** *76*, 6893-6899.

[23] R. A. Meulenbroek, K. L. Sargent, J. Lunde, B. J. Jasmin, R. J. Parks, *Mol. Ther.* **2004,** *9*, 617-624.

[24] L. P. Le, H. N. Le, I. P. Dmitriev, J. G. Davydova, T. Gavrikova, S. Yamamoto, D. T. Curiel, M. Yamamoto, *J. Natl. Cancer Inst.* **2006,** *98*, 203-214.

[25] H. Ugai, M. Wang, L. P. Le, D. A. Matthews, M. Yamamoto, D. T. Curiel, *J. Mol. Biol.* **2009**.

[26] M. Y. Nakano, U. F. Greber, *J. Struct. Biol.* **2000,** *129*, 57-68.

[27] L. Wen, Y. Lin, Z. H. Zheng, Z. L. Zhang, L. J. Zhang, L. Y. Wang, H. Z. Wang, D. W. Pang, *Biomaterials* **2014,** *35*, 2295-2301.

[28] F. Zhang, Z. Zheng, S. L. Liu, W. Lu, Z. Zhang, C. Zhang, P. Zhou, Y. Zhang, G. Long, Z. He, D. W. Pang, Q. Hu, H. Wang, *Biomaterials* **2013,** *34*, 7506-7518.

[29] Y. Zhang, X. Ke, Z. Zheng, C. Zhang, Z. Zhang, F. Zhang, Q. Hu, Z. He, H. Wang, *ACS Nano.* **2013,** *7*, 3896-3904.

[30] Y. Zhao, S. L. Lo, Y. Zheng, D. H. Lam, C. Wu, M. Y. Han, S. Wang, *Biochem. Biophys. Res. Commun.* **2013,** *434*, 110-116.

[31] J. Hao, L. L. Huang, R. Zhang, H. Z. Wang, H. Y. Xie, *Anal. Chem.* **2012,** *84*, 8364-8370.

[32] S. L. Liu, Z. Q. Tian, Z. L. Zhang, Q. M. Wu, H. S. Zhao, B. Ren, D. W. Pang, *Biomaterials* **2012,** *33*, 7828-7833.

[33] P. Zhang, S. Liu, D. Gao, D. Hu, P. Gong, Z. Sheng, J. Deng, Y. Ma, L. Cai, *J. Am. Chem. Soc.* **2012,** *134*, 8388-8391.

[34] S. L. Liu, Z. L. Zhang, Z. Q. Tian, H. S. Zhao, H. Liu, E. Z. Sun, G. F. Xiao, W. Zhang, H. Z. Wang, D. W. Pang, *ACS Nano.* **2012,** *6*, 141-150.

[35] H. Liu, Y. Liu, S. Liu, D. W. Pang, G. Xiao, *J. Virol.* **2011,** *85*, 6252-6262.

[36] Z. Q. Cui, Q. Ren, H. P. Wei, Z. Chen, J. Y. Deng, Z. P. Zhang, X. E. Zhang, *Nanoscale.* **2011,** *3*, 2454-2457.

[37] P. B. Yim, M. L. Clarke, M. McKinstry, S. H. De Paoli Lacerda, L. F. Pease, III, M. A. Dobrovolskaia, H. Kang, T. D. Read, S. Sozhamannan, J. Hwang, *Biotechnol. Bioeng.* **2009,** *104*, 1059-1067.

[38] K. I. Joo, Y. Lei, C. L. Lee, J. Lo, J. Xie, S. F. Hamm-Alvarez, P. Wang, *ACS Nano.* **2008,** *2*, 1553-1562.

[39] K. Kampani, K. Quann, J. Ahuja, B. Wigdahl, Z. K. Khan, P. Jain, *J. Virol. Methods* **2007,** *141*, 125-132.

[40] K. I. Joo, Y. Lei, C. L. Lee, J. Lo, J. Xie, S. F. Hamm-Alvarez, P. Wang, *ACS Nano.* **2008,** *2*, 1553-1562.

[41] K. I. Joo, Y. Fang, Y. Liu, L. Xiao, Z. Gu, A. Tai, C. L. Lee, Y. Tang, P. Wang, *ACS Nano.* **2011,** *5*, 3523-3535.

[42] F. Li, Z. P. Zhang, J. Peng, Z. Q. Cui, D. W. Pang, K. Li, H. P. Wei, Y. F. Zhou, J. K. Wen, X. E. Zhang, *Small* **2009,** *5*, 718-726.

[43] F. Lisi, P. Falcaro, D. Buso, A. J. Hill, J. A. Barr, G. Crameri, T. L. Nguyen, L. F. Wang, P. Mulvaney, *Adv. Healthc. Mater.* **2012,** *1*, 631-634.

[44] X. Li, D. Lu, Z. Sheng, K. Chen, X. Guo, M. Jin, H. Han, *Talanta* **2012,** *100*, 1-6.

[45] Q. Ma, W. Yu, X. Su, *Talanta* **2010,** *82*, 51-55.

[46] L. Chen, Z. Sheng, A. Zhang, X. Guo, J. Li, H. Han, M. Jin, *Luminescence.* **2010,** *25*, 419-423.

[47] J. Xue, H. Chen, M. Fan, F. Zhu, L. Diao, X. Chen, L. Fan, P. Li, D. Xia, *J. Oral Pathol. Med.* **2009,** *38*, 668-671.

[48] G. Wang, Y. Leng, H. Dou, L. Wang, W. Li, X. Wang, K. Sun, L. Shen, X. Yuan, J. Li, K. Sun, J. Han, H. Xiao, Y. Li, *ACS Nano.* **2013,** *7*, 471-481.

[49] X. Wang, X. Lou, Y. Wang, Q. Guo, Z. Fang, X. Zhong, H. Mao, Q. Jin, L. Wu, H. Zhao, J. Zhao, *Biosens. Bioelectron.* **2010,** *25*, 1934-1940.

[50] J. Peng, H. L. Chen, X. B. Zhu, G. F. Yang, Z. L. Zhang, Z. Q. Tian, D. W. Pang, *J. Nanosci. Nanotechnol.* **2011,** *11*, 9725-9730.

[51] H. L. Chen, J. Peng, X. B. Zhu, J. Gao, J. L. Xue, M. W. Wang, H. S. Xia, *Exp. Mol. Pathol.* **2010,** *89*, 367-371.

[52] L. Chen, Z. Qi, R. Chen, Y. Li, S. Liu, *Clin. Chim. Acta* **2010,** *411*, 1969-1975.

[53] L. Chen, X. Zhang, G. Zhou, X. Xiang, X. Ji, Z. Zheng, Z. He, H. Wang, *Anal. Chem.* **2012,** *84*, 3200-3207.

[54] L. Chen, X. Zhang, C. Zhang, G. Zhou, W. Zhang, D. Xiang, Z. He, H. Wang, *Anal. Chem.* **2011,** *83*, 7316-7322.

[55] M. Lyons, D. Onion, N. K. Green, K. Aslan, R. Rajaratnam, M. Bazan-Peregrino, S. Phipps, S. Hale, V. Mautner, L. W. Seymour, and K. D. Fisher, *Mol.Ther.* **2006,** *14*, 118-128.

[56] W. S. M. Wold, Adenovirus methods and protocols. **1999**.

[57] P. Murakami and M. T. McCaman, *Anal.Biochem.* **1999,** *274*, 283-288.

[58] G. A. Mayr, P. Freimuth, *J. Virol.* **1997,** *71*, 412-418.

[59] A. L. McNees, J. A. Mahr, D. Ornelles, L. R. Gooding, *J. Virol.* **2004,** *78*, 6955-6966.

[60] I. Dmitriev, V. Krasnykh, C. R. Miller, M. Wang, E. Kashentseva, G. Mikheeva, N. Belousova, D. T. Curiel, *J. Virol.* **1998,** *72*, 9706-9713.

[61] T. Seki, I. Dmitriev, K. Suzuki, E. Kashentseva, K. Takayama, M. Rots, T. Uil, H. Wu, M. Wang, D. T. Curiel, *Gene Ther.* **2002,** *9*, 1101-1108.

[62] J. K. Jaiswal, H. Mattoussi, J. M. Mauro, S. M. Simon, *Nat. Biotechnol.* **2003,** *21*, 47-51.

[63] S. Yin, S. Yang, Y. Shang, S. Sun, G. Zhou, Y. Jin, H. Tian, J. Wu, X. Liu, *PLoS. One.* **2013,** *8*, e63500.

[64] S. L. Liu, L. J. Zhang, Z. G. Wang, Z. L. Zhang, Q. M. Wu, E. Z. Sun, Y. B. Shi, D. W. Pang, *Anal. Chem.* **2014,** *86*, 3902-3908.

[65] N. Imelli, O. Meier, K. Boucke, S. Hemmi, U. F. Greber, *J. Virol.* **2004,** *78*, 3089-3098.

[66] K. E. McGrath, T. P. Bushnell, J. Palis, *J. Immunol. Methods* **2008,** *336*, 91-97.

[67] U. F. Greber, M. Willetts, P. Webster, A. Helenius, *Cell* **1993,** *75*, 477-486.

[68] U. F. Greber, P. Webster, J. Weber, A. Helenius, *EMBO J.* **1996,** *15*, 1766-1777.

[69] U. F. Greber, H. Kasamatsu, *Trends Cell Biol.* **1996,** *6*, 189-195.

[70] U. F. Greber, M. Suomalainen, R. P. Stidwill, K. Boucke, M. W. Ebersold, A. Helenius, *EMBO J.* **1997,** *16*, 5998-6007.

[71] M. Suomalainen, M. Y. Nakano, S. Keller, K. Boucke, R. P. Stidwill, U. F. Greber, *J. Cell Biol.* **1999,** *144*, 657-672.

[72] M. Suomalainen, M. Y. Nakano, K. Boucke, S. Keller, U. F. Greber, *EMBO J.* **2001,** *20*, 1310-1319.

[73] D. Majhen, J. Nemet, J. Richardson, J. Gabrilovac, M. Hajsig, M. Osmak, M. Eloit, A. Ambriovic-Ristov, *Virus Res.* **2009,** *139*, 64-73.

Supporting Information

Quantum Dot Labelling of Adenovirus Allows for Highly Sensitive Single Cell Flow and Imaging Cytometry

Morgan R. Herod, Robert G. Pineda, Vivien Mautner and David Onion*

Supporting Information

Quantum Dot Labelling of Adenovirus Allows for Highly Sensitive Single Cell Flow and Imaging Cytometry

Morgan R. Herod, Robert G. Pineda, Vivien Mautner and David Onion*

Experimental Section

Viruses and Biotinylation

AdGFP (ΔE1/E3 $CMV_{IE}GFP$) is a replication defective Ad5 vector, encoding eGFP under control of the CMV immediate early promoter. Wildtype (WT) Ad11 was a kind gift from Professor Gavin Wilkinson (University of Cardiff). AdpIX-GFP was a kind gift from Dr Robin Parks (Ottawa Health Research Institute) and expresses a pIX-GFP fusion protein for fluorescent tracking. AdDM-1/E2F and AdDM-1/E2F-RGD are Ad5 based gene therapy vectors with the E1A promoter replaced by an E2F promoter/Kozak sequence downstream of a SV40 late poly(A) signal and a DM-1 insulator element (generated using plasmids kindly donated by Dr Alemany). Both viruses have a splice acceptor-linked eGFP gene inserted downstream of the protein IV (fiber) gene. AdDM-1/E2F-RGD contains a cyclic RGD sequence inserted into the HI loop of the fibre gene. AdGFP and AdpIX-GFP were grown in HEK293 cells whilst Ad5, Ad11, AdDM-1/E2F and AdDM-1E2F-RGD were grown in A549 cells, all grown in Dulbecco's Modified Eagle Medium (DMEM) supplemented with 2% foetal calf serum (FCS) and GlutaMAX-1 (Invitrogen). All viruses were CsCl banded [56], titered by Picogreen assay for particle number and plaque assayed for infectivity before and after biotinylation.

For biotinylation, viruses were incubated with 10 μg/ml NHS-Biotin (Sigma, Pool, UK) for 4 hours at 20°C, unless otherwise stated. Excess NHS-Biotin was removed by dialysis against storage buffer (PBS, 10% glycerol (v/v), 500 μM $MgCl_2$, 900 μM $CaCl_2$) for 16 hours at 4°C.

Cell Preparation and Qdot Labelling

A549, HEK293 and SKOV3 cells were obtained from the ATCC (Manassas, VA, USA). A9 and A9-CAR cells were kindly donated by Dr Paul Freimuth (Brookhaven National Laboratory).[58] SKOV-CAR cells were generated by transfection with the pXLNC-hCAR retrovirus as has been described previously.[59] All cells were grown in DMEM supplemented with 10% foetal calf serum and GlutaMAX-1 (Invitrogen).

For virus Qdot labelling, cells were trypsinised, trypsin neutralised by addition of excess full growth media, washed (PBS supplemented with 5% FCS) before the cell suspension was incubated with excess streptavidin, washed and incubated with excess biotin (Endogenous Biotin Blocking kit, Invitrogen, Paisley, UK). Cells were washed and each sample resuspended in 50μl PBS supplemented with 5% FCS. Virus was bound to cells on ice for 90 minutes, washed, re-suspended in 50 μl PBS + 5% FCS containing 1 μl of Qdot655-Streptavidin conjugate (Invitrogen). Cells were incubated for 30 minutes on ice, washed and either analysed directly or co-stained with antibodies.

Confocal Microscopy

For confocal microscopy cells were grown on glass cover slips and prepared as above

Cells were grown on cover slips (Fisher Scientific, Loughborough, UK) and prepared as above but without cell detachment by trypsinisation. Cells were stained with 5 μg anti-CAR mAb RmCb (Cancer Research UK, UK) (20 minutes at 4°C), visualised with secondary anti-

mouse Qdot525 (Invitrogen) and counter-stained with 0.5 μg/ml DAPI (Sigma) (10 minutes at 4°C). Cells were mounted in Clarion Mounting Media (Sigma) and visualised using a Zeiss LSM510 meta confocal microscope.

Flow Cytometry

Where indicated cells in suspension were co-stained with 5 μg anti-CAR mAb RmCb (20 minutes at 4ºC) and detected using anti-mouse FITC secondary antibody (Invitrogen), following manufacturer's instructions. Data was collected using a LSR II flow cytometer (BD Bioscience, San Jose, CA, USA) equipped using a 488nm laser 530/30nm band-pass filter (for FITC and GFP) and a 405nm laser 655/8nm band-pass filter (for Qdot655). Data was analysed using FlowJo software (Tree Star, Ashland, OR, USA). Statistical analysis was performed using Graph Pad Prism 6, using paired T Test and significance indicated as *P<0.05 , **P<0.005, ***P<0.0005.

Imaging Cytometry

Cells were suspended at 10^6/ml in PBS + 5% FCS and data acquired using an Image Stream 100 (Amnis, Seattle, US) with excitation at 488 nm (30 mW) and 405 nm (350 mW). Analysis was performed on single cell in focus events, identified by brightfield aspect ratio/area analysis and brightfield gradient RMS. To measure internalisation of Qdot labelled virus, default total cell masks were used to calculate total cell fluorescence and the area erode tool (brightfield channel) used to identify cell interiors. Internalisation index (defined by the percentage of interior cell fluorescence:total cell fluorescence) was calculated and expressed as percentage of maximum internalisation. Data analysis was performed with Ideas Software (Amnis, Seattle, WA, USA).